Available online at www.sciencedirect.com
ScienceDirect
Toxicology 247 (2008) 6–10
TOXICOLOGY
www.elsevier.com/locate/toxicol

Increase in intracellular free/bound NAD[P]H as a cause of Cd-induced oxidative stress in the $HepG_2$ cells

M.S. Yang [a,*], D. Li [b], T. Lin [a], J.J. Zheng [b], W. Zheng [b], J.Y. Qu [b,**]

[a] *Department of Biology, Hong Kong Baptist University, Kowloon, Hong Kong, China*
[b] *Department of Electronic & Computer Engineering, Hong Kong University of Science and Technology, Clearwater Bay, Kowloon, Hong Kong, China*

Received 10 December 2007; received in revised form 23 January 2008; accepted 23 January 2008
Available online 7 February 2008

Abstract

The present study shows the use of confocal autofluorescence spectroscopy coupled with the time-resolved fluorescence decay analysis to measure changes in FAD/NAD[P]H and free/bound NAD[P]H in $HepG_2$ cells at 0.5, 1.5, 3 and 4.5 h after exposure to cadmium chloride (Cd). These changes were compared to changes in GSSG/GSH and production of reactive oxygen radicals (ROS) production. The results demonstrated that both FAD/NAD[P]H and GSSG/GSH increased significantly upon exposure to Cd. The change in GSSG/GSH occurred as early as 1.5 h after treatment while the change in FAD/NAD[P]H did not occur until 3 h after exposure. Production of ROS was also increased at 1.5 h. The ratio of free/bound NAD[P]H was studied. It was demonstrated that free/bound NAD[P]H increased significantly as early as 0.5 h and remained elevated until 4.5 h after treatment with Cd. The present study provides novel data to show that changes in NAD[P]H metabolism precedes the increase in ROS production and cellular oxidative stress (increase GSSG/GSH, FAD/NAD[P]H). It is suggested that Cd causes a release of NAD[P]H, an important cofactor for electron transfer, from its normal protein binding sites. This may result in a disruption of the activity of the enzyme and proteins, and may lead to the subsequent toxic events.

Keywords: Cadmium; $HepG_2$ cells; FAD/NAD[P]H; GSSG/GSH; ROS; Oxidative stress

1. Introduction

Cd is a toxic metal that has been extensively studied. The metal can bind to proteins, damage DNA and interfere with mitochondrial energy production (Muller and Ohnesorge, 1984; Liu and Liun, 1990; Al Nasser, 2000; Waalkes, 2000; Lopez et al., 2003). One of the major events in Cd-induced cell death is the change in intracellular redox state (Shih et al., 2004; Watjen and Beyersmann, 2004; Yang et al., 2004). Using $HepG_2$ cells as a model, previous studies in our laboratory demonstrated that Cd causes a dose-dependent decrease in intracellular GSH/GSSG (Yang et al., 2004), which may reflect a change in intracellular NADPH/NADP (Yang et al., 2006). However, there has been no experimental study to examine changes in intracellular NAD[P]H level upon exposure to Cd.

Nicotinamide adenine dinucleotides (NAD[P], NAD[P]H) and flavin adenine dinucleotides (FAD, $FADH_2$) are important electron transfer couples for enzymatic reactions. NAD[P]H and FAD possess intrinsic fluorescence property which renders them detectable after being excited with light of specific wavelength (Chance et al., 1962; Galeotti et al., 1970; Huang et al., 2002; Wu and Qu, 2005). The development of confocal fluorescence spectroscopy makes it possible to measure FAD and NAD[P]H simultaneously in cells (Huang et al., 2002; Rocheleau et al., 2004). The ratio of FAD/NAD[P]H has been used to reflect redox state in cells and tissues (Zhang et al., 2004). Coupled with the time-resolved fluorescence decay analysis, it is possible to study the ratio of free/bound NAD[P]H in cells (Vishwasrao et al., 2005; Wu et al., 2006), and to evaluate metabolism of these molecules in regulating redox functions. In the present study, the confocal autofluorescence spectroscopy together with the time-resolved fluorescence decay analysis were used to evaluate the changes of FAD/NAD[P]H ratio and the free/bound NAD[P]H in $HepG_2$ cells following exposure to Cd.

* Corresponding author. Tel.: +852 3411 7058; fax: +852 3411 5995.
** Corresponding author. Tel.: +852 2363 9460.
E-mail addresses: msyang@hkbu.edu.hk (M.S. Yang), eequ@ust.hk (J.Y. Qu).

0300-483X/$ – see front matter © 2008 Elsevier Ireland Ltd. All rights reserved.
doi:10.1016/j.tox.2008.01.021

2. Materials and methods

2.1. Chemicals

Cadmium chloride (Cd), GSH, GSSG, *o*-phthaladehyde (OPT), glutathione reductase (GR), cadmium chloride, $NADP^+$, NADPH, 5,5-dithiobis-2-nitrobenzoic acid (DTNB), *N*-ethylmaleimide (NEM) were from Sigma Chemical Co. (St. Louis, MO, U.S.A.). Antibiotics (amphotericin B and penicillin–streptomycin) and phosphate buffered saline (PBS) were from Life Technologies (Gibco, Grand Island, NY). Minimum essential medium (MEM), fetal bovine serum (FBS) and fungizone were obtained from Invitrogen Corp. (Scotland, UK). 2′,7′-Dichlorodihydrofluorescein diacetate (H_2DCFDA) were from Molecular Probes, Inc. (New Jersy, U.S.A.). All other chemicals used were of analytical grade and purchased from Fisher Scientific (Fair Lawn, NJ). A stock solution of Cd used for preparing the test medium was prepared by dissolving the chloride salt in double-distilled water (Millipore).

2.2. Cell culture and treatment

The $HepG_2$ cell line was purchased from American Type Culture Collection (U.S.A.) and cultured in MEM supplemented with 10% FBS, 0.5% antibiotics and 0.5% fungizone. Cells were cultured in a humidified atmosphere of 95% air and 5% CO_2 to >90% confluence. By analyzing the concentration-dependent change in cell viability, previous study in our laboratory showed that cadmium chloride (Cd) at 0.6 mM causes a 50% cell death after 3 h incubation (Yang et al., 2004). The 3 h time provides a convenient window to trace the metabolic changes during the progression of cell death. Experiments were conducted at 0.5, 1.5, 3 and 4.5 h after treatment with Cd (0.6 mM).

2.3. The set-up for measuring autofluorescence

The basic set-up used for detecting fluorescence signals from cells was similar to that described previously (Wu and Qu, 2005). Specifically, the excitation source (365 nm) was the second harmonic generation of a pulsed Ti:Sapphire laser (Mira 900-S, Coherent). The laser beam was driven by two galvanometric mirrors in order to scan the sample in the $x \pm y$ plane perpendicular to the optical axis. A water immersion objective lens (40× and NA = 1.15) of the fluorescence microscope was used to focus the excitation beam into the sample and to collect the backscattered fluorescence signals. A 100 μm optical fiber was used as a pinhole to collect the confocal fluorescence signals to the detection system. The excitation and fluorescence lights were separated by a dichroic mirror. The intensity of the fluorescence signals were analyzed by a spectrometer and recorded by a cooled-CCD camera with 5-s acquisition time. In the time-resolved measurement, the decay of fluorescence signals at a series of wavelengths ranging from 454 to 466 nm were analyzed using a time-correlated single photon counter (TCSPC) with 30-s acquisition time. The measured signals were the average fluorescence signals over a sampling area of 100 μm × 100 μm. The excitation power used was maintained at 40 μW to avoid photobleaching.

2.4. Analysis of FAD/NAD[P]H and free/bound NAD[P]H in cultured cells

Cells (1×10^6) were cultured on a coverslip (Marienfeld Laboratory Glassware, Germany) that was placed in a 35 mm Petri-dish (Iwaki, Japan) and covered with 1 ml medium containing 0.6 mM Cd. At the designated time after Cd exposure, the coverslip was removed, rinsed with pre-warmed PBS and placed under the fluorescence microscope. The analysis was completed within 20 min after cells were removed from the incubator. In the time-resolved measurement, the decay of autofluorescence from the $HepG_2$ cells following treatment. As the peak of the NAD[P]H emission spectra is about 460 nm (Wu et al., 2006), analysis was focused on the channels capturing the signals from 454 to 466 nm. The fitting analysis was based on the iterative nonlinear least squares deconvolution (Wu et al., 2006) and calculated by a dual-exponential function, $A_1 \exp(-t/\tau_1) + A_2 \exp(-t/\tau_2)$, where A_1 and A_2 are the amplitudes of the short and long lifetime components, respectively. Because the fluorescence lifetime of intracellular NAD[P]H molecules that exist in bound and free forms are inherently different, the long lifetime component (τ_2) carries information of bound NAD[P]H while the short lifetime component (τ_1) represents that of free NAD[P]H. The ratio of A_1/A_2 represents the free/bound NAD[P]H. Signals from 10 separate sites, with the minimum spacing of 200 μm between sites, were collected per dish for calculating the average of a sample. The mean and standard deviation for each treatment were calculated from the average value of 2–4 replicates using the Student's *t*-test. Treatments were considered significantly different from the control at $p < 0.05$.

2.5. Analysis of GSSG/GSH and reactive oxygen species (ROS) production

At the time of the study, the treated cells (1×10^6) were rapidly washed with PBS and extracted with 0.3 M perchloric acid (Yang and Gupta, 2003). After centrifugation to remove any particulates, the cell extract was neutralized with potassium hydroxide, and the precipitated potassium perchlorate was removed by centrifugation. GSH and GSSG were analyzed from the supernatant by the fluorometric method as described in Hissin and Hilf (1976) using *o*-phthaladehyde. The levels of GSH and GSSG were calculated from standard curves constructed from standard GSH and GSSG. The accuracy of the GSH standard was measured with DTNB, using a molar extinction coefficient of 13,600 with an absorbance of 412 nm (Eyer and Podhradsky, 1986). GSSG was standardized by measuring the decline of NADPH in the presence of glutathione reductase, taking into consideration that the molar extinction coefficient of NADPH to be 6270 at 340 nm and 1 M of NADPH converts 1 M of GSSG to 2 M of GSH (Akerboom and Sies, 1981).

Cellular ROS production was quantified by flow cytometer (Brandt and Keston, 1965; Cathcart et al., 1983). Briefly, cells were cultured in 6-well plates at a density of 1×10^6 cells per well. Thirty minutes prior to the experiment, 20 μl H_2DCFDA (1 mM) was added. In the presence of ROS, H_2DCFDA was converted to its fluorescence product, dichlorodihydrofluorescein (DCF). At the end of the experiments, cells were washed twice with pre-warmed PBS and trypsinized. After centrifugation, cells were re-suspended in PBS and passed through the FACScan flow cytometer. Fluorescence intensities of DCF-stained cells were analyzed using the CellQuest™ software (Becton Dickinson, FACScan).

3. Results

Fig. 1 shows the time-course of changes in FAD/NAD[P]H in $HepG_2$ cells following exposure to Cd. The results demonstrated that changes in FAD/NAD[P]H ratio occurred at 3 and 4.5 h after Cd exposure. There was no significant change in this ratio at 0.5 and 1.5 h when compared to untreated cells. Cells appeared as a monolayer (Fig. 1, inserts a and b) until 3 h (c) after treatment with Cd. At 4.5 h, the appearance of cells (d) changed but adequate number of attached cells was still available for analysis.

GSSG/GSH is a common index that reflects cellular redox state. Fig. 2 shows that similar to FAD/NAD[P]H, there was a significant increase in GSSG/GSH ratio after exposure to Cd. The change was significant at 1.5 h. Fig. 3 shows that there was an increase in cellular ROS production. The increase was significant at 1.5, 3 and 4.5 h after Cd exposure. These results consistently show that oxidative stress occurs at 1.5 h after Cd exposure. Changes in GSSG/GSH and ROS production occurs prior to changes in FAD/NAD[P]H.

The fluorescence lifetime for NAD[P]H was measured and the ratio of the amplitudes of two lifetime components A_1/A_2 were studied. At resting state, the decay constants for τ_1 and τ_2 were 0.3–0.4 ns and 2–3 ns, respectively. There were no significant changes in these parameters after Cd treatment (Table

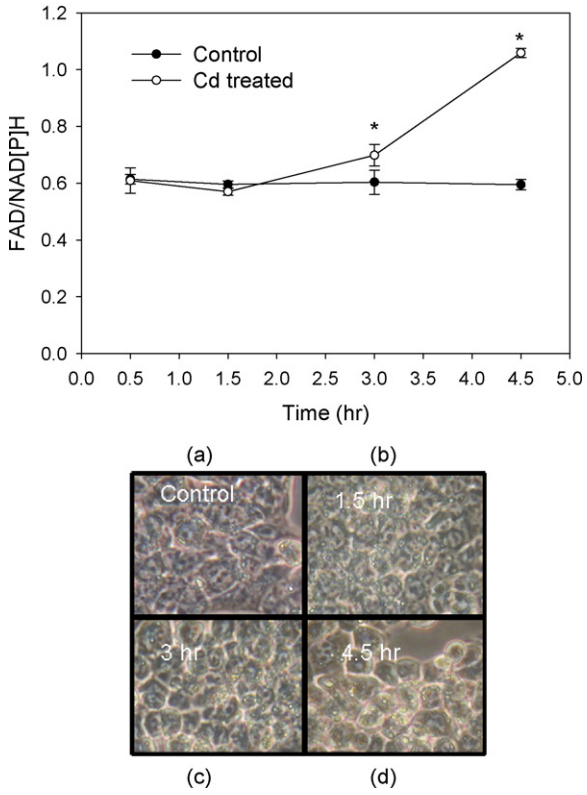

Fig. 1. FAD/NAD[P]H ratio in $HepG_2$ cells at different time points after treatment with 0.6 mM Cd. Each value represents the mean and S.D. of four sets of experiments. * indicates that the value is significantly different ($p < 0.05$) from that of the corresponding control. Inserts (a–d) are micrographs (40×) of cells taken at different time points.

1), indicating that the emitted lights were characteristic to that under control at all times. However, the ratio of A_1/A_2 increased significantly as the time of treatments increased (Fig. 4). There was a 37% increase in the A_1/A_2 as early as 0.5 h after treatment with 0.6 mM Cd. The increase reached over twofold at 3 h, and approximately fourfold of that of control cells after 4.5 h treatment. The result demonstrated that the level of free NAD[P]H (short lifetime component) was significantly increased relative to the bound NAD[P]H (long lifetime component) in cells.

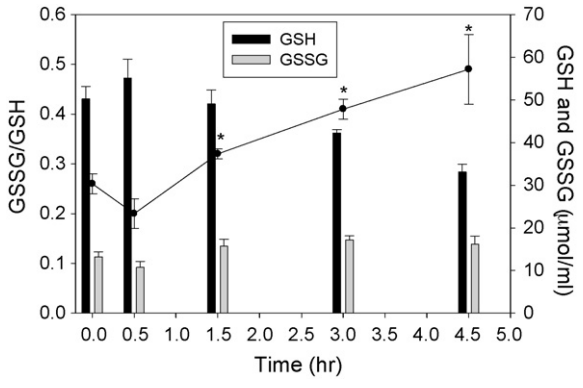

Fig. 2. Analysis of GSH, GSSG and GSSG/GSH ratio in $HepG_2$ cells at different time after treatment with 0.6 mM Cd. Each value represents the mean and S.D. of four sets of experiment. * indicates that the value of GSSG/GSH is significantly different ($p < 0.05$) from that of the control at 0 h.

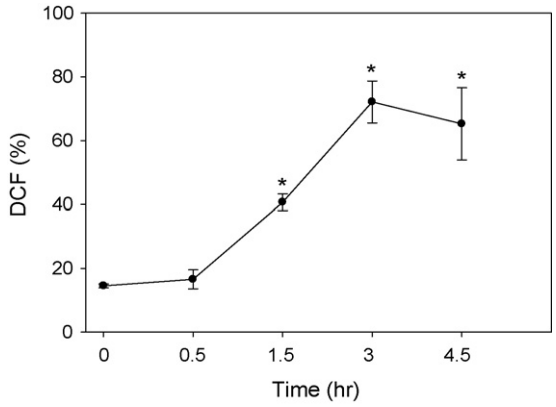

Fig. 3. Analysis of free radical production in $HepG_2$ cells after exposure to Cd. Each value is the mean and S.D. of three replicates. * indicates that the value is significantly different ($p < 0.05$) from that of the control at 0 h.

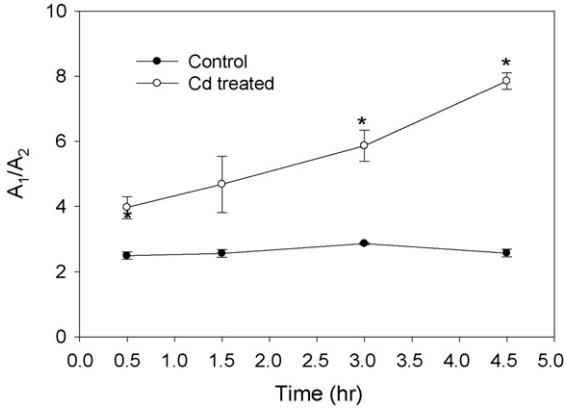

Fig. 4. Time course of change in the ratio of free/bound NAD[P]H (A_1/A_2) in the $HepG_2$ cells after exposure to 0.6 mM Cd. The ratio of free vs. bound levels was obtained from the decay of the NAD[P]H fluorescence emission at the wavelength from 454 nm to 466 nm. The fluorescence decay curve was calculated by a dual-exponential function, $A_1 \exp(-t/\tau_1) + A_2 \exp(-t/\tau_2)$. Each value is the mean and S.D. of two sets of experiments, each obtained with an average of 10 independent records. * indicates that the value is significantly different ($p < 0.05$) from that of the control. The following table shows that the decay constants (τ_1 and τ_2) were not different at the different time points after Cd treatment.

Treatment time (h)	τ_1 (ns)	τ_2 (ns)
0	0.33 ± 0.06	2.71 ± 0.42
0.5	0.35 ± 0.05	2.90 ± 0.23
1.5	0.32 ± 0.04	2.52 ± 0.24
3	0.34 ± 0.05	2.68 ± 0.58
4.5	0.36 ± 0.04	2.74 ± 0.48

4. Discussion

Cd is one of the most toxic environmental pollutants known to cause cancer and cell death. The basic mechanism of the action of Cd is not well understood. Previous studies in our laboratory demonstrated that exposure of HepG2 and the C6 glioma cells to Cd resulted in a decrease in intracellular GSH/GSSG (Yang et al., 2004). Using three independent redox indicators, FAD/NAD[P]H (Fig. 1), GSSG/GSH (Fig. 2) as well as ROS production (Fig. 3), the present study further confirmed that

oxidative stress occurred. Time course study demonstrated that GSSG/GSH ratio (Fig. 2) and ROS production (Fig. 3) were significantly increased at 1.5 h and FAD/NAD[P]H was not significantly increased until 3 h after Cd exposure. These events were preceded by a change in free/bound NAD[P]H, which occurred as early as 0.5 h. Thus, the results demonstrated that oxidative stress may be a consequence of NAD[P]H metabolism. Consistently, previous study using the same experimental model showed that there was a significant increase in intracellular NADH and a corresponding decrease in NAD^+ as early as 0.5 h in this cell line (Yang et al., 2008). While it is difficult to distinguish NADH and NADPH using the current analytical method (Bennett et al., 1996), fluorescence images obtained by the current method usually represents change of both NADH and NADPH and denoted by NAD[P]H (Rocheleau et al., 2004). The corresponding change in NADH and NAD^+ in previous study would indicate that a change in NADH (and NADPH) and NAD^+ (and $NADP^+$) interconversion rather than an increase in synthesis of NAD[P]H. NAD[P]H and $NAD[P]^+$ are important electron carriers for many enzymatic reactions. A change in their interconversion may reflect a disruption in the activity of these enzymes. Thioredoxin reductase, glutathione reductase, phosphoglycerate dehydrogenase, NADH Coenzyme Q reductase, mitochondria glycerol-3-phosphate dehydrogenase, biliverdin reductase A as well as the nucleoside diphosphate linked moiety and mitochondrial apoptosis inducing factor (AIF) (HomoloGene link database for human cells, Pubmed) are enzymes known to bind to NAD[P]H. In the case of glutathione reductase, recent study by Tandogan and Ulusu (2007) showed that Cd can inhibit its activity in yeast. Although it is not clear how the inhibition reaction occurred, it is possible that Cd displaces NAD[P]H from this enzyme and interferes with its ability to carry out the reduction reaction. A reduced in glutathione reductase activity might gradually lead to an accumulation of GSSG and thus an increase in GSSG/GSH.

Besides glutathione reductase, another interesting protein that requires attention is the mitochondrial AIF, a flavoprotein with NADH oxidase activity that also acts as a powerful antioxidant in the mitochondria (Modjtahedi et al., 2006). In mammalian cells, AIF is released in response to proapoptotic members of the bcl-2 family and translocates to the cell nucleus where it binds to DNA, resulting in chromosome condensation and caspase-independent apoptosis (Cande et al., 2004; Modjtahedi et al., 2006). AIF is closely associated with the mitochondrial electron transport chain (Modjtahedi et al., 2006). In Harlequin (Hq) mouse deficient in AIF (to 10–20% wild type level), there were functional defects in the oxidative phosphorylation complexes I and III in brain and retina, resulting in significant reduction in ATP generation and organ degeneration (Vahsen et al., 2004). Cd-induced apoptosis occurs via activation of caspases (Oh and Lim, 2006). Using the present experimental model, Yang et al. (2008) showed that majority of the events associated apoptosis including caspase activation, reduction in ATP production and appearance of apoptotic cells occurred at various time points after 1.5 h. Thus, the signaling pathway for Cd-induced apoptosis is associated with caspase activation and not AIF translocation. Nevertheless, whether there was a release in NAD[P]H from this protein and whether this event may be related to other mitochondrial events associated with apoptosis require further investigation.

In the present study, the time course of changes showed that prior to oxidative stress, there was a change in NAD[P]H metabolism. To further demonstrate that the change in redox state may not be the primary event of Cd-induced toxicity, studies using the LLC-PK_1 kidney cells (Wispriyono et al., 1998) or the C6 glioma cells (Yang et al., 2007) showed that improvement of intracellular GSH/GSSG by pretreatment with NAC, a molecule capable of improving intracellular GSH/GSSG, was unable to protect against Cd-induced death unless NAC was applied simultaneously with the toxic metal. The results suggested that the efficacy of NAC may not be due to the change in intracellular redox state, but to the ability of NAC to prevent Cd from binding to cellular organelles (Yang et al., 2007). In conclusion, the study demonstrated that upon Cd exposure, NAD[P]H, an important cofactor for electron transfer, is released from its normal protein binding sites. It can be hypothesized that this change may cause a disruption of the activity of the enzymes and/or proteins, and may lead to subsequent toxic events. Furthermore, experiment in the present study was conducted with a concentration of Cd that causes 50% cell death after 3 h of exposure. Cd has been shown to cause DNA damage at concentration much lower than this level (Waalkes, 2000). In subsequent study, research should be carried out to study changes in NAD[P]H binding and the impact of NAD[P]H release upon exposure to sublethal concentration of Cd.

Acknowledgements

The study was supported by the Faculty Research Grant from the Hong Kong Baptist University. Lin was supported by the postgraduate research grant from the Research Grant Council, Hong Kong.

References

Akerboom, T.P., Sies, H., 1981. Assay of glutathione, glutathione disulfide, and glutathione mixed disulfides in biological samples. Methods Enzymol. 77, 373–382.

Al Nasser, I.A., 2000. Cadmium hepatotoxicity and alterations of the mitochondrial function. J. Toxicol. Clin. Toxicol. 38, 407–413.

Bennett, B.D., Jetton, T.L., Ying, G., Magnuson, M.A., Piston, D.W., 1996. Quantitative subcellular imaging of glucose metabolism within intact pancreatic islets. J. Biol. Chem. 271, 3647–3651.

Brandt, R., Keston, A.S., 1965. Synthesis of diacetyldichlorofluorescin: a stable reagent for fluorometric analysis. Anal. Biochem. 11, 6–9.

Cande, C., Vahsen, N., Garrido, C., Kroemer, G., 2004. Apoptosis-inducing factor (AIF): caspase-independent after all. Cell Death. Differ. 11, 591–595.

Cathcart, R., Schwiers, E., Ames, B.N., 1983. Detection of picomole levels of hydroperoxides using a fluorescent dichlorofluorescein assay. Anal. Biochem. 134, 111–116.

Chance, B., Cohen, P., Jobsis, F., Schoener, B., 1962. Intracellular oxidation–reduction states in vivo. Science 137, 499–508.

Eyer, P., Podhradsky, D., 1986. Evaluation of the micromethod for determination of glutathione using enzymatic cycling and Ellman's reagent. Anal. Biochem. 153, 57–66.

Galeotti, T., van Rossum, G.D., Mayer, D.H., Chance, B., 1970. On the fluorescence of NAD(P)H in whole-cell preparations of tumours and normal tissues. Eur. J. Biochem. 17, 485–496.

Hissin, P.J., Hilf, R., 1976. A fluorometric method for determination of oxidized and reduced glutathione in tissues. Anal. Biochem. 74, 214–226.

Huang, S., Heikal, A.A., Webb, W.W., 2002. Two-photon fluorescence spectroscopy and microscopy of NAD(P)H and flavoprotein. Biophys. J. 82, 2811–2825.

Liu, R.M., Liun, Y.G., 1990. Effects of cadmium on the energy metabolism of isolated hepatocytes: its relationship with the nonviability of isolated hepatocytes caused by cadmium. Biomed. Environ. Sci. 3, 251–261.

Lopez, E., Figueroa, S., Oset-Gasque, M.J., Gonzalez, M.P., 2003. Apoptosis and necrosis: two distinct events induced by cadmium in cortical neurons in culture. Br. J. Pharmacol. 138, 901–911.

Modjtahedi, N., Giordanetto, F., Madeo, F., Kroemer, G., 2006. Apoptosis-inducing factor: vital and lethal. Trends Cell Biol. 16, 264–272.

Muller, L., Ohnesorge, F.K., 1984. Cadmium-induced alteration of the energy level in isolated hepatocytes. Toxicology 31, 297–306.

Oh, S.H., Lim, S.C., 2006. A rapid and transient ROS generation by cadmium triggers apoptosis via caspase-dependent pathway in HepG2 cells and this is inhibited through *N*-acetylcysteine-mediated catalase upregulation. Toxicol. Appl. Pharmacol. 212, 212–223.

Rocheleau, J.V., Head, W.S., Piston, D.W., 2004. Quantitative NAD(P)H/flavoprotein autofluorescence imaging reveals metabolic mechanisms of pancreatic islet pyruvate response. J. Biol. Chem. 279, 31780–31787.

Shih, C.M., Ko, W.C., Wu, J.S., Wei, Y.H., Wang, L.F., Chang, E.E., Lo, T.Y., Cheng, H.H., Chen, C.T., 2004. Mediating of caspase-independent apoptosis by cadmium through the mitochondria-ROS pathway in MRC-5 fibroblasts. J. Cell Biochem. 91, 384–397.

Tandogan, B., Ulusu, N.N., 2007. The inhibition kinetics of yeast glutathione reductase by some metal ions. J. Enzyme Inhib. Med. Chem. 22, 489–495.

Vahsen, N., Cande, C., Briere, J.J., Benit, P., Joza, N., Larochette, N., Mastroberardino, P.G., Pequignot, M.O., Casares, N., Lazar, V., Feraud, O., Debili, N., Wissing, S., Engelhardt, S., Madeo, F., Piacentini, M., Penninger, J.M., Schagger, H., Rustin, P., Kroemer, G., 2004. AIF deficiency compromises oxidative phosphorylation. EMBO J. 23, 4679–4689.

Vishwasrao, H.D., Heikal, A.A., Kasischke, K.A., Webb, W.W., 2005. Conformational dependence of intracellular NADH on metabolic state revealed by associated fluorescence anisotropy. J. Biol. Chem. 280, 25119–25126.

Waalkes, M.P., 2000. Cadmium carcinogenesis in review. J. Inorg. Biochem. 79, 241–244.

Watjen, W., Beyersmann, D., 2004. Cadmium-induced apoptosis in C6 glioma cells: influence of oxidative stress. Biometals 17, 65–78.

Wispriyono, B., Matsuoka, M., Igisu, H., Matsuno, K., 1998. Protection from cadmium cytotoxicity by *N*-acetylcysteine in LLC-PK1 cells. J. Pharmacol. Exp. Ther. 287, 344–351.

Wu, Y., Qu, J.Y., 2005. Two-photon autofluorescence spectroscopy and second-harmonic generation of epithelial tissue. Opt. Lett. 30, 3045–3047.

Wu, Y., Zheng, W., Qu, J.Y., 2006. Sensing cell metabolism by time-resolved autofluorescence. Opt. Lett. 31, 3122–3124.

Yang, M.S., Gupta, R.C., 2003. Determination of energy charge potential in the C6 glioma and the HepG-2 cell culture. Toxicol. Mech. Methods 13, 97–101.

Yang, M.S., Yu, L.C., Gupta, R.C., 2004. Analysis of changes in energy and redox states in HepG2 hepatoma and C6 glioma cells upon exposure to cadmium. Toxicology 201, 105–113.

Yang, M.S., Chan, H.W., Yu, L.C., 2006. Glutathione peroxidase and glutathione reductase activities are partially responsible for determining the susceptibility of cells to oxidative stress. Toxicology 226, 126–130.

Yang, M.S., Yu, L.C., Pat, S.W., 2007. Manipulation of energy and redox states in the C6 glioma cells by buthionine sulfoxamine and *N*-acetylcysteine and the effect on cell survival to cadmium toxicity. Cell. Mol. Biol. 53, 56–61.

Yang, M.S., Lin, T, Li, D., Qu, J.Y., 2008. Analysis of intracellular NADH level in the HepG2 cells and its relation with cellular energy level and cell death following acute cadmium exposure. In: Collery, P., Theophanides, T., Maymard, I., Collery, T. (Eds.), Metal. Ions Biol. Med., vol 10, John Libbey Eurotext, Paris, in press.

Zhang, Z., Blessington, D., Li, H., Busch, T.M., Glickson, J., Luo, Q., Chance, B., Zheng, G., 2004. Redox ratio of mitochondria as an indicator for the response of photodynamic therapy. J. Biomed. Opt. 9, 772–778.